Mol. Cryst. Liq. Cryst., Vol. 544: pp. 69/[1057]–76/[1064], 2011

ISSN: 1542-1406 print/1563-5287 online
DOI: 10.1080/15421406.2011.569275

Taylor & Francis
Taylor & Francis Group

Study of Optical Bounce According to Electrode Structure in the Fringe-Field Switching Mode Using the Negative Liquid Crystal

KYUNG SU HA,[1] PANKAJ KUMAR,[1] CHANG WOO WOO,[1] WAN-SEOK KANG,[2] GI-DONG LEE,[2] AND SEUNG HEE LEE[1]

[1]Department of BIN Fusion Technology and Department of Polymer Nano-Science and Technology, Chonbuk National University, Jeonju, Jeonbuk, Korea
[2]Department of Electronics Engineering, Dong-A University, Pusan, Korea

The switching response behavior of negative dielectric anisotropic liquid crystal in the fringe-field switching (FFS) mode was investigated with respect to the pixel electrode positions. When the applied voltage relaxes to lower voltage, optical bounce was observed at the edge region of pixel electrode. Based on the simulation results, we have proposed a promising molecular behavior associated with optical bounce, which originates from the reorientation process of LC director that is in over-twist state associated with tilt angle. Experimental results also show the optical bounce during switching-off time.

Keywords Electrode structure; fringe-field switching; liquid crystal; negative dielectric anisotropy; optical bounce; response time

1. Introduction

In recent years, liquid crystal displays (LCDs), owing to their low operating voltage, lightweight and thinness,are being widely used for all kinds of displays replacing cathode-ray tube (CRT) displays. However, still LCDs need to be improved in image quality compared to CRTs. LCDs use a viscous liquid crystal (LC) with birefringence, so that the response time of the device is rather slow and its image quality changes according to the viewing direction. In order to improve viewing angle dependency of image qualities, various advanced LC devices such as multi-domain vertical alignment (MVA) [1–3], patterned vertical alignment (PVA) [4,5], in-plane switching (IPS) [6–9] and fringe-field switching (FFS) [10–15] modes were developed.

Address correspondence to Gi-Dong Lee, Department of Electronics Engineering, Dong-A University, Pusan 607-735, Korea. Tel.: +82-63-270-2343; Fax: +82-63-270-2341; E-mail: gdlee@dau.ac.kr and Seung Hee Lee, Department of BIN Fusion Technology and Department of Polymer Nano-Science and Technology, Chonbuk National University, Jeonju, Jeonbuk, Korea. E-mail: lsh1@chonbuk.ac.kr

Consecutively to improve the response time of LCDs, several researchers proposed numerous solutions such as over driving [16,17] and high frame frequency [18–20] methods. With increase in frame hertz (Hz), faster response time of LC or LC mode needs to be developed. Among all above, the FFS mode is known to exhibit high light efficiency, wide viewing angle and low operating voltage, simultaneously.

In this paper, we have studied the molecular reorientation in detail, during field-off switching in the FFS mode when LC with negative dielectric anisotropy (−LC) is used. In vigilantly inspecting the switching responses, we found that there is an optical bounce appeared at the edge region of pixel electrode after turn off the applied electric field. Generally, the optical bounce is a complicate phenomenon that has been reported to be resulted from many kinds of mechanisms, such as backflow effect, ion screen effect, etc. [21–23]. However, in the FFS mode, simulated and experimental results reveal that the optical bounce phenomenon results from the reorientation process of LC director that is in over-twist at the edge of pixel electrode. In order to solve the problems, molecular orientation according to electrode structure was performed and the solution is proposed to minimize the optical bounce phenomena.

2. Switching Principle and Simulation Conditions

Figure 1 shows the side view of schematic cell structure and orientation of the LCs in off and on states in the FFS cell using −LC. In the FFS mode, the electrodes exist onlyat the bottom substrate. In general, common electrodes existas plane and pixel electrodes exist in slit form with suitable gaps (l) between them. With this electrode structure, afringe-electric field with both horizontal (E_y) and vertical (E_z) field components is generated when voltage is appliedand, more importantly, a strong E_y exists near the bottom surface at the edge of each pixel electrode. The LCs are homogeneously aligned in an initial state, in which the optic axis of the LC is co incident with one of the crossed polarizer axis. The field rotates LC and thus LC director deviates from polarizer axis, giving rise to transmittance.

In the FFS mode using a −LC, the LC orientation in white state are strongly dependent on electrode positions and thus two types of light modulation, phase retardation like in the IPS mode and polarization rotation like in the twisted nematic (TN) are mixed, depending on electrode positions [24–26]. As a result, the

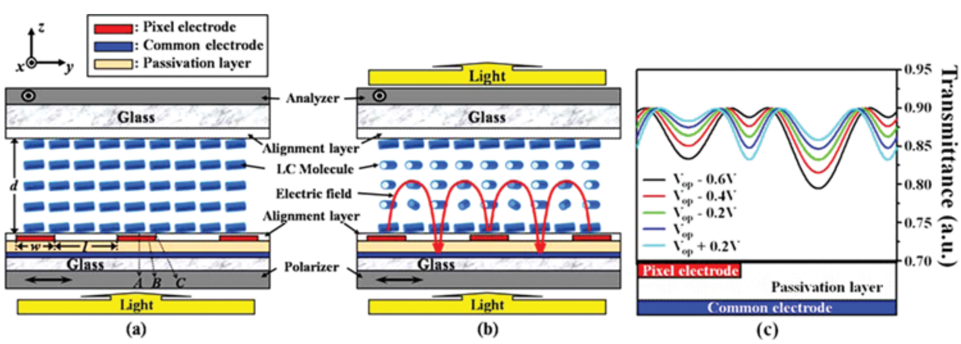

Figure 1. Schematic cell structure with molecular orientation in the fringe-field switching mode; (a) Off state, (b) On state, (c) Transmittance distribution along with electrodes position at different applied voltages. (Figure appears in color online.)

normalized light transmission in the FFS mode using a −LC is determined by the following equation

$$T/T_0 = \alpha \sin^2(2\varphi)\sin^2(\beta\pi d\Delta n_{eff}/\lambda) + \gamma\left(1 - \frac{\sin^2(\pi/2)\sqrt{1+(2\delta d\Delta n_{eff}/\lambda)^2}}{1+(2\delta d\Delta n_{eff}/\lambda)^2}\right) \quad (1)$$

where α, β, γ, and δ are fitting parameters, φ is an angle between LC director and transmission axes of the crossed polarizer, d is a cell gap, Δn_{eff} is a voltage-dependent effective birefringence of LC medium, and λ is the wavelength of the incident light.

We performed a simulation using "LCD master" (Shintech, Japan) where the motion of LC directors and optical transmittance calculation were based on Eriksen-Leslie theory and extended 2×2 Jones Matrix [27]. In the computer simulation, the width of pixel electrode (w), l and d were 3 μm, 4.5 μm and 4 μm, respectively. Here, the LC having physical properties (dielectric anisotropy $\Delta\varepsilon = -4.0$, $\Delta n = 0.09$, elastic constants $K_{11} = 13.5$ pN, $K_{22} = 6.5$ pN, and $K_{33} = 15.1$ pN) were used. In order to define LC molecular orientations according to the pixel electrode positions, center, between, and edge regions of pixel electrode were named as position *A*, *B*, and *C* respectively (see Fig. 1(a)). The strong anchoring at both substrates with anchoring energy much larger than $10^{-3}\,\mathrm{Jm}^{-2}$ is assumed such that the LCs at the interface are strongly anchored and donot rotate. The calculated LC orientation in this paper is achieved after relaxation time of 100 ms.

To understand the voltage-transmittance characteristic along electrodes positions in more detail, we investigated the electrode-position dependent transmittance under the different applied voltages, for instance, below operating voltage (V_{op}) which shows maximal transmittance, at V_{op} and above V_{op}, as shown in Figure 1(c). When the applied voltage is less than 0.6 V of V_{op}, the transmittance is almost maximal at the edge of pixel electrode (position *C*) but it is quite low at the center of electrode (position *A*). With increasing applied voltage up to V_{op}, the transmittance at electrode position *C* decreases while it increases at electrode position *A*, reaching maximal transmittance overall. When the applied voltage exceeds V_{op} by 0.2 V, the transmittance at electrode position *C* decreases while it increases slightly at electrode position *A*, resulting in slight decrease in overall transmittance compared to that at V_{op}. The difference in transmittance along electrode positions indicate that the V_{op} is not constant along the electrode position, instead, it is electrode-position dependent. Therefore, when the applied field is turned-off, optical bounce in time-dependent transmittance could be occurred.

3. Simulation Results and Discussion

To confirm the characteristics of response time in the FFS device, time-dependent transmittance according to the electrode positions was calculated as shown in Figure 2. At the position *C*, large optical bounce which gives the response time slower was monitored. In order to verify how long the response time delays after removing the electric field, time-dependent transmittance was more specifically studied, as shown in Figure 2. Among all the pixel electrode positions, the largest optical bounce observed at position *C* holds up the response time for 6 ms. On the

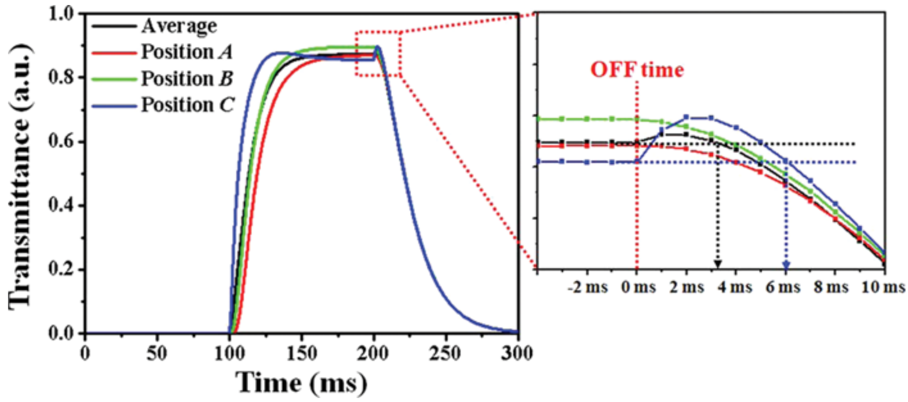

Figure 2. Time-dependent transmittance with respect to pixel electrode positions and detail LC relaxation process after turn off voltage.

other hand, optical bounce is not observed at position *A* and *B*. Nevertheless, overall time-dependent transmittance shows the optical bounce during turn-off.

To understand the origin of the decreased transmittance, the transmittance along the electrode position is calculated after removing the electric field, as shown in Figure 3. As clearly indicated in the magnified data in the dotted regions, the transmittance at the electrode positions *A* and *B*, decreases after turning off the electric fields, that is, no optical bounce is observed.On the other hand, the transmittance at position *C* increases slightly up to additional 2 ms after turning off the electric fields.

Figure 4 shows time-resolved twist and tilt profile of LCs with respect to the pixel electrode positions after removing the electric field.As shown in Figure 4(a–f); the twist and tilt angle of LC directors at position *A*, *B* and *C*, decreased after turning off the electric fields. The average optical bounce observed considering all the pixel electrode positions holds up the response time for 3.2 ms. However, among

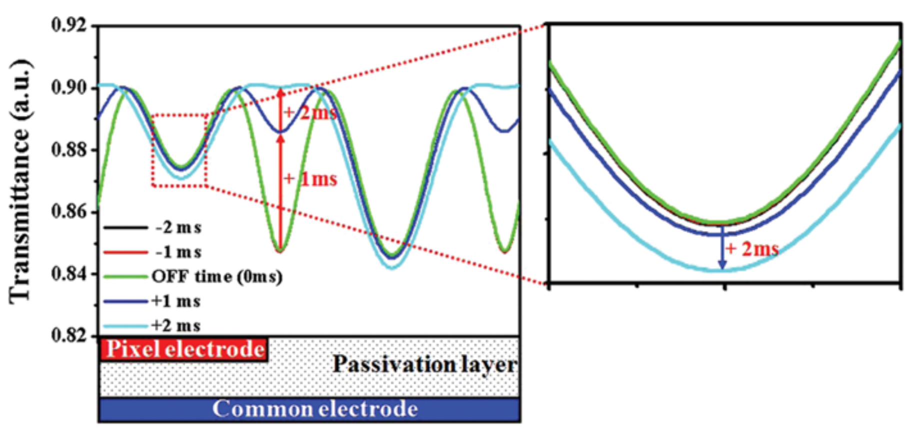

Figure 3. Change of transmittance along electrodes according to the relaxation time during decaying.

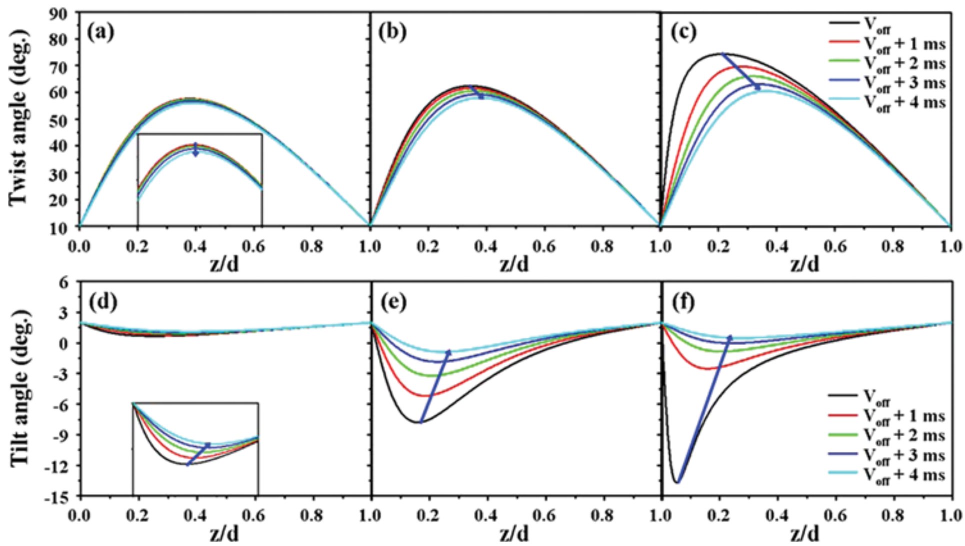

Figure 4. Time-dependent twist/ tilt angle with respect to pixel electrode positions*A*(a, d), *B* (b, e) and *C*(c, f).

the pixel electrode positions, the optical bounce at position *C* holds up the response time for 6 ms. At electrode positions *A* and *B*, twist and tilt angle decreases continuously so that φ and $d\Delta n_{eff}$ would decrease without causing any optical bounce. Even at the electrode position *C*, both twist and tilt seem to decrease after turning-off the applied voltage. However, detail observation brings up another story that position of the maximal twist angle changes, that is, from z/d = 0.225 at turn-off voltage to z/d = 0.375 at 4 ms later after turn-off time. This implies that the light modulation method changes from polarization rotation at the beginning to phase retardation at 4 ms later, and on other hand, the tilt angle also decreases abruptly after turn-off, which is associated with the fact that K_{11} and K_{33} is much larger than K_{22}, resulting faster relaxation in bend and splay deformation than in twist. The decrease of tilt angle means that the $d\Delta n_{eff}$ at normal direction increases instead of monotonic decrease unlike LC molecular reorientation at positions *A* and *B*. The molecular profile indicates clearly that although the maximal twist angle decreases after turn-off time, the light modulation becomes phase retardation at position *C* and the effective retardation there could reach $\lambda/2$ phase to exhibit maximal transmittance even 4 ms later after turn-off time.

From understandings of switching principle of the FFS mode and molecular relaxation process after turn-off, one can understand that the optical bounce of the FFS mode with –LC comes from overtwist of LC director in turn-on state to achieve maximal transmittance overall and also faster tilt relaxation than twist one due to difference in magnitude of elastic constants, near the edge of electrode. Therefore, if the applied voltage is less than V_{op}, we expect that the optical bounce would decrease because the level of overtwist is diminished and tilt angle is less larger in the lower voltage than that in V_{op}. Figure 5 shows time-dependent transmittance during turn-on and – off time as a function of applied voltages. When V_{op} (4.7 V) is applied, strong optical bounce during turn-off process is observed at position *C* (see

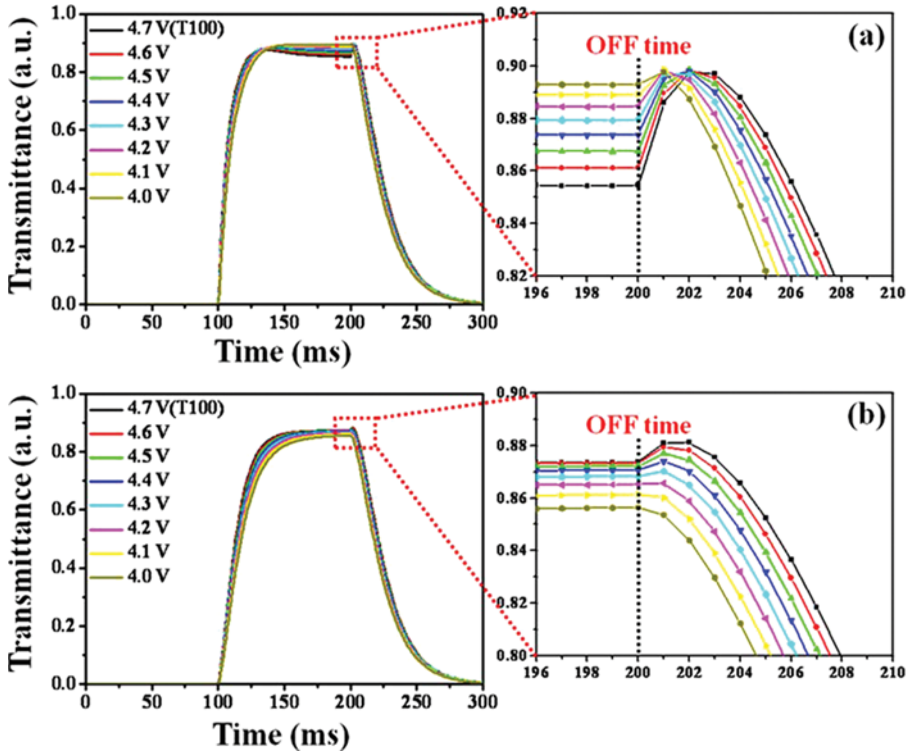

Figure 5. Time-dependent transmittance exhibiting detail time-reolved transmittance after removing the electric fields (decaying time) according to operating voltage. (a) Position *C*, (b) All region.

Fig. 5(a)), and its level decreases with decreasing applied voltage. When the voltage reaches 4.0 V, the optical bounce is almost suppressed. When considering all electrode regions, the optical bounce becomes weaker with decreasing voltage and it is almost suppressed at 4.2 V (see Fig. 5(b)), confirming our assumption.

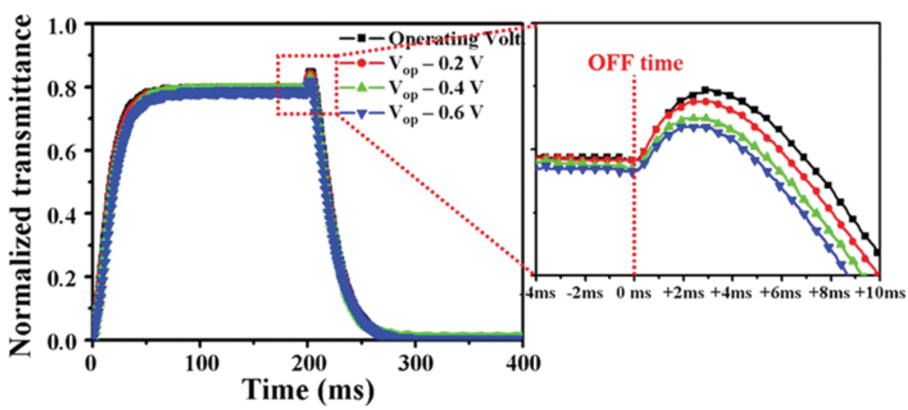

Figure 6. Time-dependent transmittance as a function of applied voltages with detail LC relaxation process after turn off voltage.

In order to assure the above hypotheses under this proposed low voltage scheme, we studied the optical bounce experimentally in FFS mode using −LC. The cell structure and physical properties of LC are similar to those in calculated results. Response time was measured by an optic system "LCMS-200" (Sesim Photonics Technology, Korea) according to applied voltages, as shown in Figure 6. As indicated, the level of optical bounce decreases when the applied voltage becomes smaller than V_{op}, and in addition, it is almost suppressed when the applied voltage is reduced by −0.6 V from $V_{op.}$ As a result, the experimental outcomes confirm well the simulated consequences.

4. Conclusions

In this paper, time-dependent transmittance and orientation of LCs have been studied in the FFS mode by using the negative dielectric anisotropic liquid crystals as a function of pixel electrode positions based on computer simulation and experiment. In the FFS mode, we can reduce the optical bounce with decreasing operating voltage because the optical bounce was caused by over twist of LC molecule and faster relaxation of bend/splay deformation than that of twist deformation at the edge region of pixel electrode. As a result, homogeneously aligned FFS mode can improve the slow response time with minimizing the optical bounce by means of optimizing driving voltage. The experimental outcomes confirm well the simulated consequences.

Acknowledgment

This work was supported by Merck Advanced Technology Korea and the World Class University program (R31-20029) funded by the Ministry of Education, Science and Technology.

References

[1] Clerc, J. F. (1991). *SID Int. Symp. Dig. Tech. Pap.*, *22*, 758.
[2] Ong, H. L. (1992). *SID Int. Symp. Dig. Tech. Pap.*, *23*, 405.
[3] Lee, S. H., Kim, H. Y., Park, I. C., Rho, B. G., Park, J. S., Park, H. S., & Lee, C. H. (1997). *Appl. Phys. Lett.*, *71*, 2851.
[4] Kim, K. H., Lee, K., Park, S. B., Song, J. K., Kim, S., & Souk, J. H. (1998). *Proc. 18th Int. Display Research Conf. (Asia Display)*, 383.
[5] Lee, H., Park, S. H., Lee, M.-H., Oh, S. T., & Lee, G.-D. (2005). *Appl. Phys. Lett.*, *86*, 031108.
[6] Kiefer, R., Weber, B., Windsceid, F., Baur, G. (1992). *In Proceedings of the 12th International Display Research Conference*, Hamamatsu, Japan, *547*.
[7] Oh-e, M., & Kondo, K. (1995). *Appl. Phys. Lett.*, *67*, 3895.
[8] Jung, B. S., Baik, I. S., Song, I. S., Lee, G.-D., & Lee, S. H. (2006). *Liq. Cryst.*, *33*, 1077.
[9] Lee, J.-H., Choi, S.-W., Kim, K.-M., Lee, G.-D., Choi, H. C., Lee, S. H., & Kim, J. C. (2007). *Mol. Cryst. Liq. Cryst.*, *478*, 99.
[10] Lee, S. H., Lee, S. L., & Kim, H. Y. (1998). *Appl. Phys. Lett.*, *73*, 2881.
[11] Lee, S. H., Lee, S. L., & Kim, H. Y. (1998). *Proc. 18th Int. Display Research Conf. (Asia Display)*, 371.
[12] Lee, S. H., Lee, S. M., Kim, H. Y., Kim, J. M., Hong, S. H., Jeong, Y. H., Park, C. H., Choi, Y. J., Lee, J. Y., Koh, J. W., & Park, H. S. (2001). *SID Int. Symp. Dig. Tech. Pap.*, *32*, 484.

[13] Lee, S. H., Kim, H. Y., Lee, S. M., Hong, S. H., Kim, J. M., Koh, J. W., Lee, J. Y., & Park, H. S. (2002). *J. Soc. Inf. Disp.*, *10*, 224.
[14] Ryu, J. W., Lee, J. Y., Kim, H. Y., Park, J. W., Lee, G.-D., & Lee, S. H. (2008). *Liq. Cryst.*, *35*, 407.
[15] Jung, J. H., Ha, K. S., Srivastava, A. K., Lee, H. K., Lee, S.-E., & Lee, S. H. (2010). *J. K. Phys. Scie.*, *56*, 548.
[16] Cho, Y., Park, C., Bhowmik, A., & Lee, S.-W. (2010). *Optical Engineering*, *49*, 034001.
[17] Gwag, J. S., Kim, J. C., & Yoon, T.-H. (2006). *Jpn. J. Appl. Phys.*, *45*(9A), 7047.
[18] Berkeley, B. H., & Hulyalkar, S. N. (2008). *SID Int. Symp. Dig. Tech. Pap.*, *39*, 358.
[19] Kim, T., Ye, B., Vu, C. P., Balram, N., & Steemers, H. (2008). *SID Int. Symp. Dig. Tech. Pap.*, *39*, 362.
[20] Kim, S. S., You, B. H., Choi, H., Berkeley, B. H., Kim, D. G., & Kim, N. D. (2009). *SID Int. Symp. Dig. Tech. Pap.*, *40*, 424.
[21] Chen, S.-H., & Chen, L.-Y. (1999). *Appl. Phys. Lett.*, *75*, 3491.
[22] Chen, P.-L., & Chen, S.-H. (2000). *Jpn. J. Appl. Phys.*, *39*, L297.
[23] Jeon, S. Y., Shin, S. H., Lee, J.-H., Lee, S. H., & Lee, Y. H. (2007). *Jpn. J. Appl. Phys.*, *46*, 7801.
[24] Schadt, M., & Helfrich, W. (1971). *Appl. Phys. Lett.*, *18*, 127.
[25] Takano, H., Suzuki, S., & Hatoh, H. (1992). *IBM J. Res. Dev.*, *36*, 23.
[26] Jung, S. H., Kim, H. Y., Lee, M.-H., Rhee, J. M., & Lee, S. H. (2005). *Liq. Cryst.*, *32*, 267.
[27] Lien, A. (1990). *Appl. Phys. Lett.*, *57*, 2767.